

Received October 30, 2019, accepted November 12, 2019, date of publication November 15, 2019, date of current version December 2, 2019.

Digital Object Identifier 10.1109/ACCESS.2019.2953818

# Pyramidal Optical Flow Method-Based Lightweight Monocular 3D Vascular Point Cloud Reconstruction

CHANG LIU<sup>1</sup>, ZHAO ZHANG<sup>1</sup>, HUANGXING LIN<sup>2</sup>, YAQIONG HU<sup>3</sup>, EYK NG<sup>4</sup>,  
DANGZHAO CHEN<sup>1</sup>, LEI ZHAO<sup>5</sup>, YIFAN LU<sup>5</sup>, XIN DAI<sup>1</sup>, SHIPU XU<sup>6</sup>,  
XIAOJUN LIU<sup>7</sup>, AND NING XIE<sup>5</sup>

<sup>1</sup>School of Information Technology, Nanchang Hangkong University, Nanchang 330063, China

<sup>2</sup>Fujian Key Laboratory of Sensing and Computing for Smart City, School of Informatics, Xiamen University, Xiamen 361005, China

<sup>3</sup>Department of Cardiology, Shanghai East Hospital, Shanghai 200120, China

<sup>4</sup>School of Mechanical and Aerospace Engineering, Nanyang Technological University, Singapore 639798

<sup>5</sup>Center for Future Media, School of Computer Science and Engineering, University of Electronic Science and Technology of China, Chengdu 611731, China

<sup>6</sup>Agricultural Information Institute of Science and Technology, Shanghai Academy of Agricultural Sciences, Shanghai 201403, China

<sup>7</sup>Mathematical and Information Engineering Department, Nanhu College of Jiaying University, Jiaying 314001, China

Corresponding authors: Yaqiong Hu (huyaqiong161@163.com), Shipu Xu (xushipu39706879@163.com), Xiaojun Liu (xjliu1204@126.com), and Ning Xie (seanxiening@gmail.com)

This work was supported by Nanchang Hangkong University's seventh batch of innovation and entrepreneurship education curriculum cultivation project "Virtual Reality Technology and Application" (No. kcpy1910).

**ABSTRACT** We propose a method for reconstructing a 3D point cloud of the organ model based on optical flow and take the 3D cardiovascular model reconstruction as an example. This optical-flow distribution based 3D point cloud reconstruction method is divided into four steps. Firstly, we employ the Coey filter to remove the noise points and improve the resolution of the raw images. Secondly, we implement the Shi-Tomasi method to extract the feature points from these filtered images. Thirdly, we remove the redundancy in the feature point set by the optical flow distributions. Finally, we converted the obtained feature points from 2D to 3D through the optical flow distribution and then reconstructed a 3D point cloud of the medical organ. With the help of our 3D representation, doctors and patients can view the 3D medical models on the Web. The final result on the Web shows the proposed method is feasible and superior.

**INDEX TERMS** 3D point cloud, 3D medical digital representation, coronary angiography, Web3D, lightweight, optical flow.

## I. INTRODUCTION

As the number one cause of death globally, cardiovascular disease (CVD) has been widely concerned. According to data provided by WHO, an estimated 17.9 million people died from CVDs in 2016, representing 31% of all global deaths [1]. In recent years, a large amount of visual data has been obviously applied to the diagnosis and treatment of CVD, such as magnetic resonance angiography [2], optical coherence tomography (OCT) [3], coronary angiography [4], and so on. Though most of these visual data represented by 2D video images exhibit a high resolution, they all have flaws. First of all, high-resolution video images have produced a huge amount of data, which not only incurs a high data-storage burden for hospital but also challenges telemedicine with high transmission efficiency requirements.

The associate editor coordinating the review of this manuscript and approving it for publication was Yongtao Hao.

Secondly, 2D video images are limited by the camera's view-point and angle, so accidental blind area can't be avoided. Thirdly, these data are not intuitive to the patients. Without the doctor's explanation, most of patients can't directly understand his or her illness through these data. So, we present a kind of clear, intuitive and lightweight 3D visual organ representation using a 3D point cloud, and take the 3D cardiovascular point cloud reconstruction as an example. The reconstruction method of the 3D point cloud is mainly based on optical flow, including four steps, namely noise removal, 2D feature point extraction, feature point optimization, and construction of 3D feature points, as shown in Fig. 1. Moreover, our input data is the current mainstream data, coronary angiography.

## II. RELATED WORK

Researchers have been focusing on modeling methods for 3D human organ models [5], [6]. Given the slender shape of the

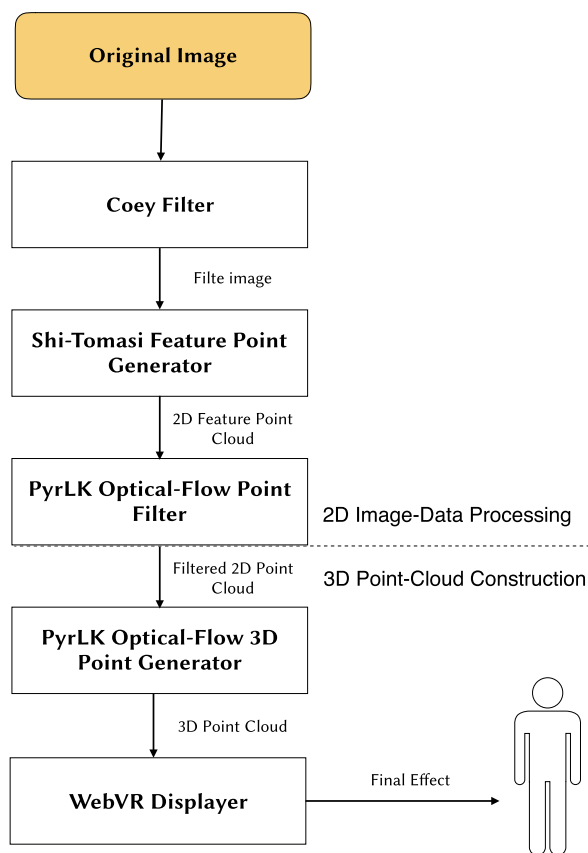


**FIGURE 1.** The pipeline of our method, includes 1) Noise removal 2) Feature points extraction 3) Error pixels removal in feature point cloud and 4) 3D point cloud reconstruction.

coronary arteries, researchers generally want to construct the basic shape or topology of the coronary arteries by extracting the centerline of the artery. The extraction of the centerline can be directly from the coronary angiogram, but the noise of the raw video images make the job very difficult. So image filters are essential throughout the modeling process. There are many filters that can be used to segment blood vessels in x-ray images [7], and some of them have been widely used [8]. Frangi filters [9] and Gabo filters [10] are two typical representatives of classic filters. The preferred filter for 3D coronary artery reconstruction is either one of these two filters, or an improvement based on it [11]. Comparing the two methods, the former is more ideal for cleaning the entire image noise, while the latter is more effective for some areas of interest. Instead of using these two filters, our method chose the Coey filter [12], which not only removes noise in the input images but also increases the resolution of the output image.

Noise filtering for the original image is the first step in an image-based 3D reconstruction method. The filtered image is often used by the researchers to extract the blood vessel boundary or centerline [13]. The next step is to convert these two-dimensional line information into a three-dimensional NURBS surface or luminal contour [14]. Although the end result looks good, the patch-based modeling approach is not

always good in dealing with occlusion problems, especially self-occlusion problems. Yet, self-occlusion problems are common in vascular modeling.

In addition to the patch, the point cloud is also a type of representation [15]. Chiastra et al. proposed a method for generating point clouds using optical coherence tomography (OCT) [16]. However, it is impossible to construct the entire coronary structure at one time with OCT. H. Khaleel et al. proposed a method for surface reconstruction of coronary artery using 3D point cloud, but their operation is complex and the final result is not satisfactory [17]. Therefore, we propose a coronary 3D representation based on PyrLK optical flow, which completes the entire 3D coronary artery reconstruction task in monocular vision.

Optical flow is used to express the motion of the pixels throughout the video stream. Optical flow method has been used in many areas such as image processing, motion detection, object segmentation, etc. Our inspiration for optical flow modeling was inspired by Zhang *et al.* [18]. They employed PyrLK optical flow method to reconstruct a three-dimensional model of a tree with similar topology to the coronary arteries.

There are three contributions in our paper, including one method and two algorithms. First of all, we present optical flow distribution based lightweight monocular 3D vascular point cloud reconstruction method. After entering a coronary angiogram, this method can reconstruct a 3D point cloud of coronary vessels. Secondly, we proposed a noise reduction algorithm for feature point extraction in coronary angiogram. This algorithm separates feature points on organs with temporal coherence from noise points without temporal coherence based on the optical flow distribution and then removes noise points. Thirdly, we proposed 3D point cloud generation algorithm. Under the assumption that the three-dimensional instantaneous moving speed of the points on the organ are similar, this algorithm constructs the relationship between the Z coordinate of the 3D point and the optical flow distribution.

### III. OVERVIEW

In this section, the overview of the proposed method is shown in Fig. 1. The pipeline of this method is divided into four steps: (i) Noise removal. In this stage, we remove the noise points in the raw images, and increase the resolution of these images. Section 4(A) presents the detail of noise removal by employing Coey filter. (ii) 2D feature point extraction. After obtaining the high-resolution filtered image, we extract the feature points from them. Section 4(B) presents the detail of the feature points extraction by using *Shi – Tomasi* method. (iii) Feature point optimization. This is the final step in preparing the input data for 3D point cloud reconstruction. In this stage, we remove the redundancy in obtained feature points, and section 5(A) show the detail. (iv) 3D point cloud reconstruction. We converted the obtained feature points from 2D to 3D, and then reconstructed a 3D point cloud of the medical organ. Section 5(B) presents the detail of 3D point cloud construction. In our technical pipeline, the first three steps that

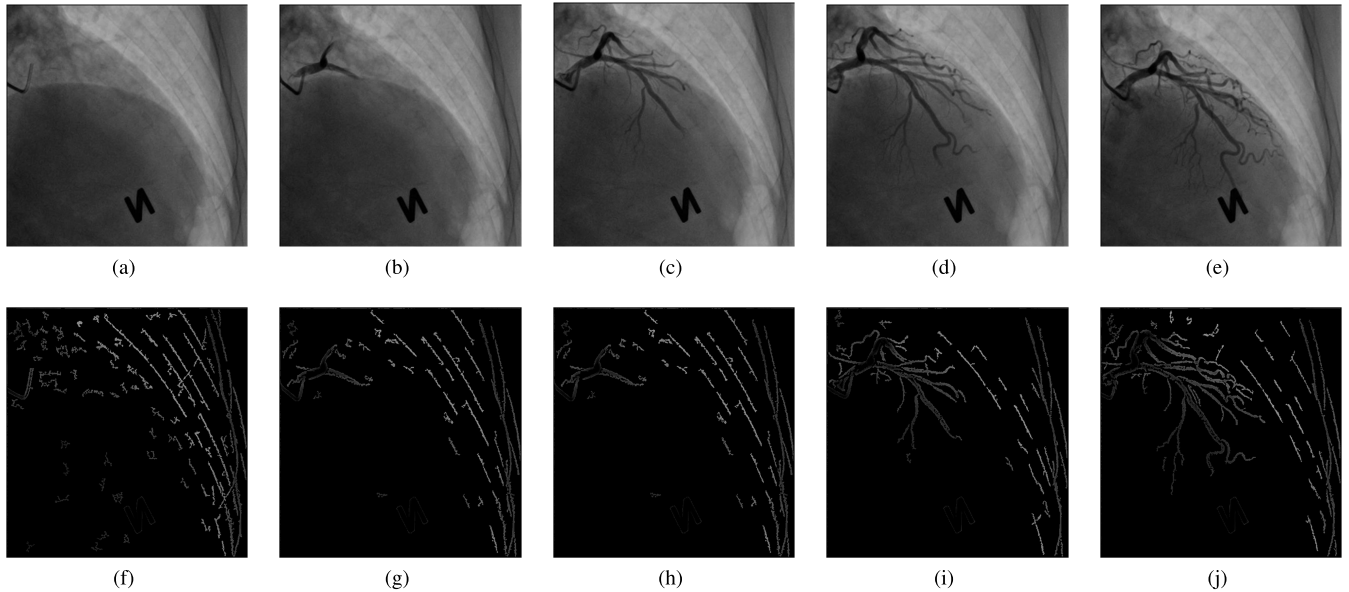


**FIGURE 2.** Original input images and their filtered image. The first row shows the original images, and the second row presents the corresponding filtered images.

prepare input data for 3D point cloud reconstruction involve noise reduction, optimization and feature extraction of 2D images, so we collectively term them 2D image-Processing phase. Furthermore, we term the last step 3D Point-Cloud Reconstruction phase.

**IV. IMAGES PROCESSING**

**A. NOISE REMOVAL BASED COEY FILTER**

Our original input images derived from a coronary angiogram contains many noise points, shown in Fig. 2(a-e). Hence, we employ Coey filter, proposed by Coey Tyler [12], to remove the noise points in these images. The entire filtering process is divided into four steps: (i) We resize the image and converts the RGB image to a grayscale image via PCA. (ii) We employ PCA again to enhance the contrast of the grayscale image. (iii) We obtain high-frequency detail information by subtracting the grayscale image and the image processed by the averaging filter; (iv) We utilizes *IsoData* method to cluster. Overall, this filter not only removes the noise points but also improves the quality of the raw images. However, the increase in image resolution often leads to more noise. So, we set a threshold value to obtain a balance between them, and the result is shown in Fig. 2(f-j).

**B. 2D FEATURE POINT EXTRACTION**

In this stage, we employed *Shi – Tomasi* method [19], which has been improved from the *Harris* method [20], to extract the feature points from the images filtered. This method is divided into four steps: (i) We compute the smaller eigen-value of each pixel’s self-adaptive matrix *M* and store it to matrix *eig*. (ii) We mark the maximum value of *eig* as *maxval* and processes the thresholds. (iii) We remove the feature points that smaller than  $quality(QualityLevel * maxval)$ .

(iv) We ensure that distance between all the corner points is higher than the least value set before. We implement *Shi – Tomasi* method by *OpenCV*.

Grayscale change Function  $E(u,v)$  presents the self-similarity of image  $(x,y)$  after translation  $(u,v)$  at the point  $(x,y)$

$$E(u, v) = \sum_{x,y} (w(x, y)[I(x + u, y + v) - I(x, y)]^2) \quad (1)$$

After being Taylor expanded, and with substitution.

$$E(u, v) \simeq [u, v] \begin{bmatrix} u \\ v \end{bmatrix} \quad (2)$$

Matrix *M* is the adaptive matrix of each pixel.

$$M = \begin{bmatrix} \sum_{s(p)} I_x^2 & \sum_{s(p)} I_x I_y \\ \sum_{s(p)} I_x I_y & \sum_{s(p)} I_y^2 \end{bmatrix} \quad (3)$$

**V. 3D POINT CLOUD RECONSTRUCTION**

In this section, the optical-flow data fulfills an important role, which is used to not only optimize the 2D feature points acquired in the previous stage but also implement 3D cloud point reconstruction, and the result is shown in Fig. 3.

**A. FEATURE POINT OPTIMIZATION**

The feature points optimized based Optical-flow method has three assumptions: (i) brightness constancy; (ii) temporal persistence; (iii) spatial coherence.

Assuming that source image is  $I(x, y, t)$ , and moved image is  $I(x + \delta x, y + \delta y, t + \delta t)$ . *T* is a higher order term that can be ignored if the movement is small enough. They satisfy

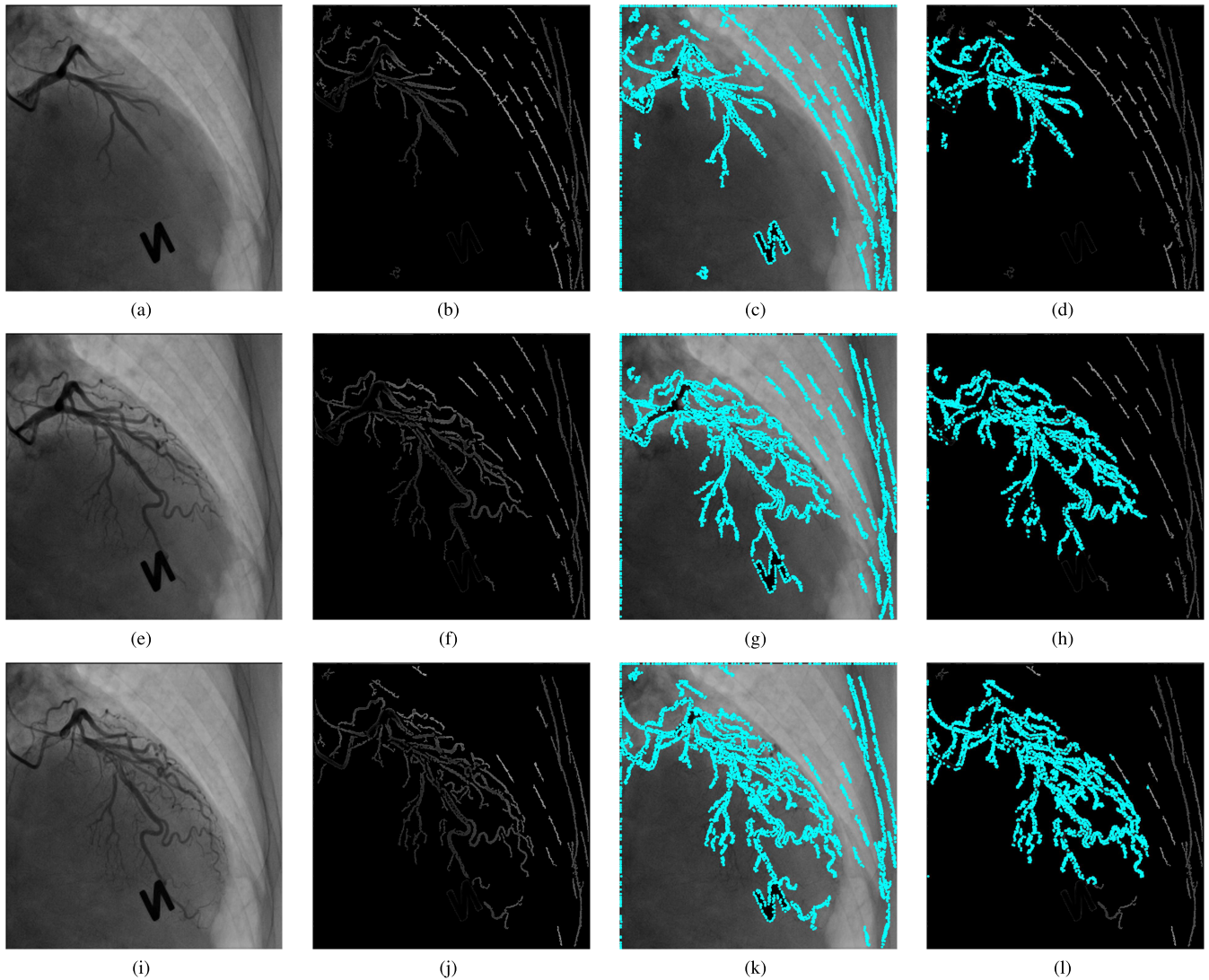


**FIGURE 3.** 2D Feature points construction process. The first column reveals the original images of coronary angiogram, the second column reveals the corresponding filtered images, the third column presents the 2D point pools generated by the filtered images, and the fourth column shows the 2D point pools created by the filtered images and then filtered by optical flow method.

equation (4).

$$I(x + \delta x, y + \delta y) = I(x, y, t) + \frac{\partial I}{\partial x} \delta x + \frac{\partial I}{\partial y} \delta y + \frac{\partial I}{\partial t} \delta t + T \quad (4)$$

Assuming that Vector  $\vec{V}(V_x, V_y)$ ,  $V_x = u$ ,  $V_y = v$ , is the composition of optical flow vector  $I(x, y, t)$ , The equation has three unknowns, which is so-called aperture problem. Assuming that optical flow  $I(V_x, V_y)$  is a constant in a small window size of  $m^3 (m > 1)$ , then from pixel  $1 \dots n$ ,  $n = m^3 (m > 1)$ , the following set of equations can be obtained equation (8),

$$\frac{\partial I}{\partial x} V_x + \frac{\partial I}{\partial y} V_y + \frac{\partial I}{\partial t} = 0 \quad (5)$$

By the equation (4) and equation (8), we can get the equation (6) using the least square method.

$$\begin{bmatrix} I_{x1} & I_{y1} \\ I_{x2} & I_{y2} \\ \vdots & \vdots \\ I_{xn} & I_{yn} \end{bmatrix} \begin{bmatrix} x \\ y \end{bmatrix} = \begin{bmatrix} -I_{t1} \\ -I_{t2} \\ \vdots \\ -I_{tm} \end{bmatrix} \quad (6)$$

Assuming that  $A\vec{V} = -b$ , then

$$\vec{V} = (A^T A)^{-1} A^T (-b) \quad (7)$$

So far, it's only the Lucas-Kanade optical flow method [20]. In contrast, Pyr Lucas-Kanade method using the multi-layer image scaling pyramid can perform smoothly even if the object moves at faster rate.

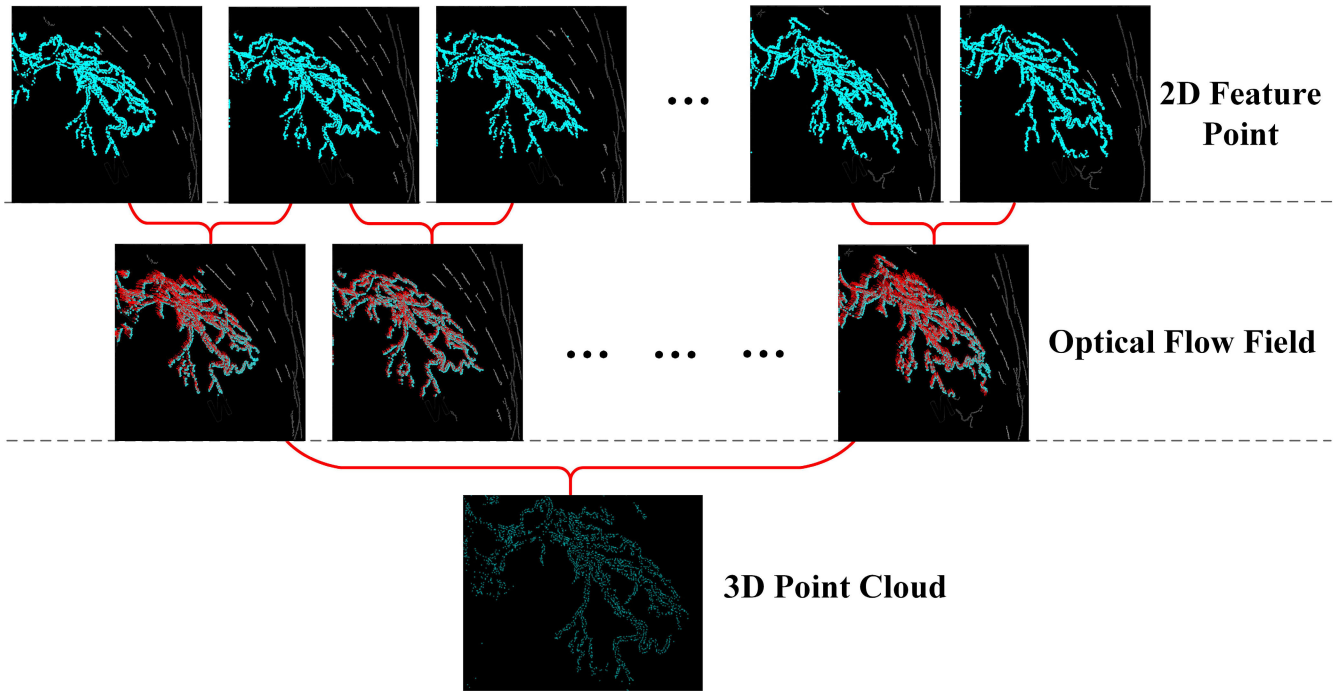


**FIGURE 4.** 3D point cloud reconstruction process. Images on the top row show the 2D feature point cloud. Images in the middle row generated by every two images on the top row are Optical-flow-field images. The bottom image is the final result of 3D point cloud.

#### Algorithm 1

**Input:** 1. *Vector* fp: feature points; 2. *Vector* npp: The PyrLK method calculates the position of the feature point in the next frame 3. *Float* minDis: minimum distance; 4. *Float* maxDis: maximum distance

```

1: for  $i = 0; i < fp.size(); i++$  do
2:    $x = (fp[i].x - npp[i].x) * (fp[i].x - npp[i].x)$ 
3:    $y = (fp[i].y - npp[i].y) * (fp[i].y - npp[i].y)$ 
4:   if  $\sqrt{x + y} < minDis$  then
5:     erase fp.begin()+i from fp
6:     erase npp.begin()+i from npp
7:      $i--$ 
8:   end if
9:   if  $\sqrt{x + y} > maxDis$  then
10:    erase fp.begin()+i from fp
11:    erase npp.begin()+i from npp
12:     $i--$ 
13:   end if
14: end for

```

The feature points are representative of the blood vessel pixels, and it is evident that the velocity changes at these points have a strong temporal correlation. Instead, the velocity of noise points is irregular. Therefore, the velocity an outstanding attribute for removing noise points. After getting the velocity of these points using the Pyr Lucas-Kanade method [21], we set a decision range for the effective feature point velocity to filter those points again, and the details is shown in Algorithm 1.

#### B. 2D POINT TRANSFER TO 3D POINT

The velocity of coronary artery movement in coronary angiography is regular and stable. This time-correlated scenario makes us boldly assume that the moving velocities of adjacent vertices at the same time are similar. From the above results, we can obtain optimized 2D feature points and their optical flow field information, as shown in Fig. 4. Based on the assumptions and known conditions, we obtain the following equation.

$$\begin{cases} x_1^2 + y_1^2 + z_1^2 = L \\ x_2^2 + y_2^2 + z_2^2 = L \\ \vdots \\ x_n^2 + y_n^2 + z_n^2 = L \end{cases} \quad (8)$$

where  $V_i(x_i, y_i, z_i) (1 \leq i \leq n)$  is the three-dimensional velocity of adjacent feature points, wherein  $x_i$  and  $y_i$  can be known by the optical-flow-field. Assuming that the three-dimensional velocity is consistent at this time, it can be inferred that the modulus lengths of the respective three-dimensional speeds are the same. It is thus possible to calculate  $z_i$  and  $L$  in this range.

According to the above results, if the difference in the moving speed of each point on the coronary aorta is negligible, the speed difference between the points in the optical flow field of the coronary angiogram is mainly due to the distance between the sampling point and the camera, that is, the depth value ( $Z$ ). In other words, the point where the speed is higher in the optical flow field is closer to the camera, and vice versa, as depicted in Algorithm 2.

**Algorithm 2**

**Input:** 1. *Vector* fp: feature points; 2. *Vector* nnp: The PyrLK method calculates the position of the feature point in the next frame 3. *Int* Size: Number of feature points 4. *Vector* speed: Optical flow distance 5. *Vector* ccp: Corresponding characteristic point 6. *Float* MaxDistance: maximum distance 7. *Vector* z: Store the z value 8. *Point2f* MaxP: Maximum distance point 9. *Int* MaxId: The id of the maximum distance point

```

1: for i = 0; i < Size; i ++ do
2:   for t = 0; t < fp.size(); t ++ do
3:     x = (fp[t].x-nnp[t].x)*(fp[t].x-nnp[t].x)
4:     y = (fp[t].y-nnp[t].y)*(fp[t].y-nnp[t].y)
5:     TempdisB = sqrt(x + y);
6:     if TempdisB > MaxDistance then
7:       MaxP = fp[t];
8:       MaxId = t;
9:       MaxDistance = TempdisB;
10:    end if
11:  end for
12:  push back MaxP to ccp
13:  push back MaxDistance to speed
14:  erase TemUse.begin()+MaxId from fp
15:  erase TemUseA.begin()+MaxId from nnp
16:  i --
17:  Size --
18:  MaxDistance =0
19: end for
20: for i = 0; i < ccp.size(); i ++ do
21:   Tempz = speed[1] - speed[i]
22:   push back Tempz to z
23: end for

```

**VI. RESULTS AND DISCUSSION**

We run our method using a desktop computer with an Intel Core i7-7700HQ processor for 8 GB of physical memory and a NVIDIA GeForce GTX 1060 GPU with 6GB of memory. The desktop runs Windows 10, and we use visual studio and MatLab as the mainly IDE. Moreover, many toolkits, such as OpenCV, Potrees and visualization toolkit (VTK) are used for the method.

**A. 2D FEATURE POINTS EXTRACTION**

We collected images from 11 different time points of the same coronary angiogram and used them as input images. As related in the Fig. 5. Even for the same coronary artery model, the feature points obtained by these input information are different. Since the original input images have low quality and many noises, the number of feature points in these images after filtering is significantly lower than in the raw images, which further confirmed the effectiveness of the filter. Besides, after filtering by the optical flow method, the number of points fell sharply again, which also proved that the optical flow method works well.

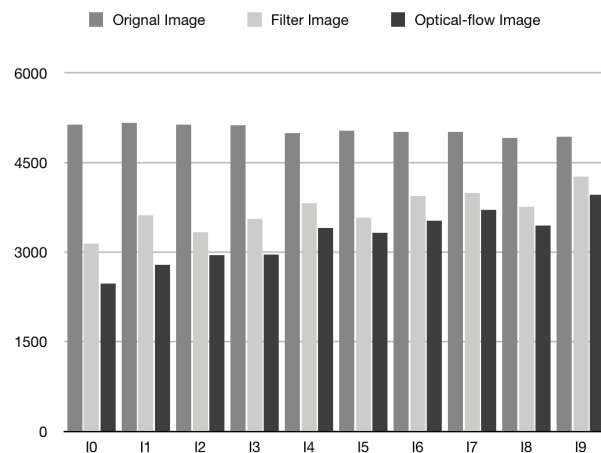


**FIGURE 5.** Comparison of the number of vertices in different images. (Original Image vs. Filter image vs. Optical-flow Image).

One of the determinant factors for the number and quality of generated 2D points is the quality level set in the Shi-Tomasi method. Fig. 6 shows the relationship of quality level and the number of these points. The smaller the quality coefficient, the higher the quality level and the greater the number of feature points.

**B. FINAL RESULT SHOW ON THE WEB**

After achieving the 3D point cloud, how to present them is very important. There are many platforms that can be used for point cloud display, such as VTK, Meshlab, 3DS Max, and so on. However, most of these application platforms are desktop-level application platforms that require configuration of the environment. Some of these tools are very unfavorable for sharing between users, and it is difficult to take advantage of the 3D point cloud. Therefore, we chose the Web3D-based Portree display platform, which makes our point cloud easy to display on the Web. In addition, the platform's powerful post-processing capabilities are ideal for sharing and interacting with users. Our final result is presented in Fig. 7.

**C. DISCUSSION**

This paper proposes a method for rapidly creating a lightweight coronary 3D point cloud model. The input of this method only requires coronary angiogram that is a kind of mainstream medical data. We have three motivations for this approach. (i) 3D point cloud data can be quickly generated by mainstream 2D medical images. (ii) The generated 3D data can be displayed on cross-platform web browser. (iii) To lay the foundation for future interactive 3D telemedicine [22]. The three-dimensional modeling method based on the above three motives has obvious advantages and disadvantages compared with the traditional coronary artery reconstruction method. The advantage is that our 3D point cloud reconstruction is faster and the generated 3D data is lighter. Our method can generate a point cloud model in less than 5 seconds and it is impossible with most of the traditional coronary artery

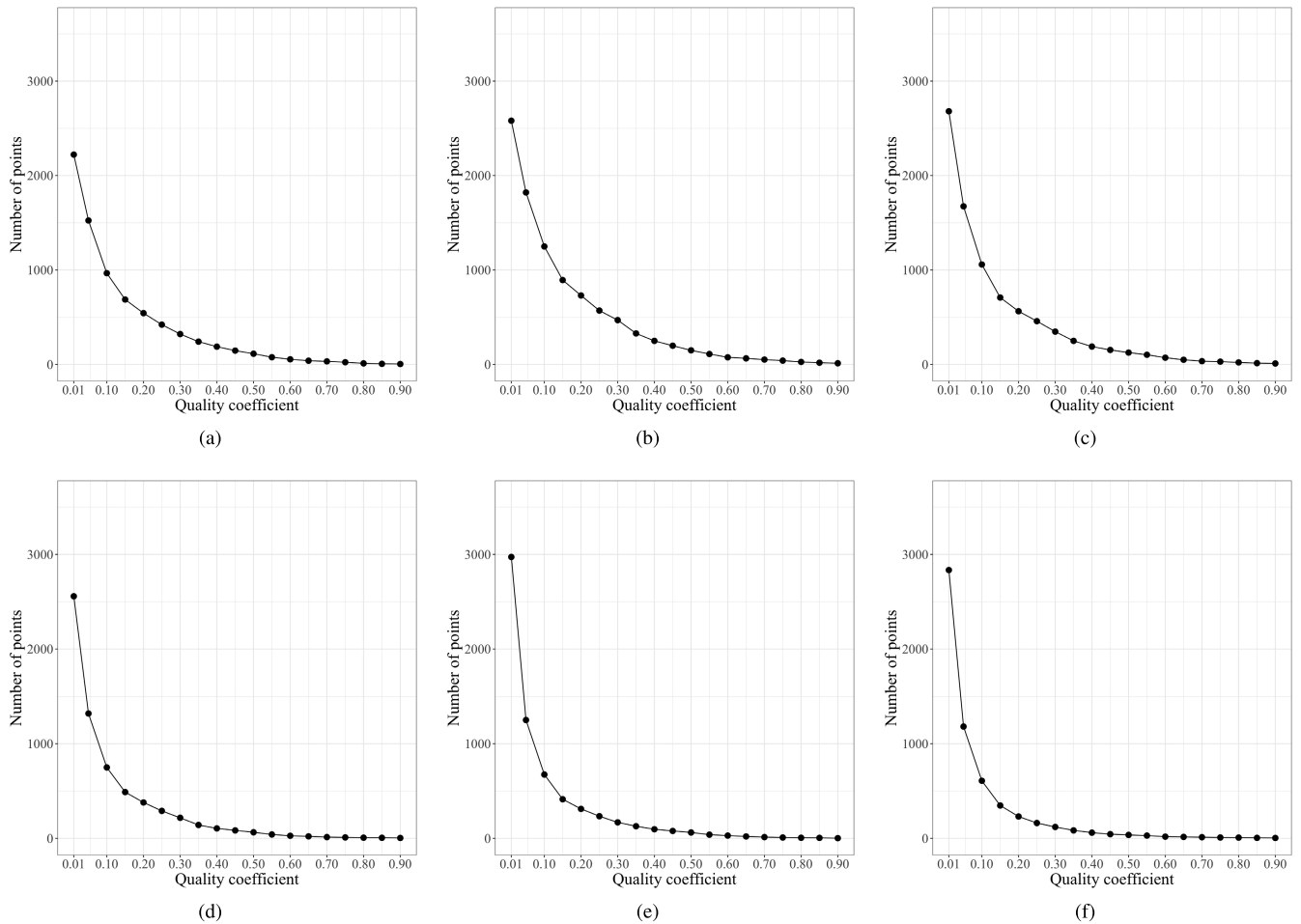


**FIGURE 6.** Relationship between 3D point cloud’s quality and its number of points. The test object is the 3D point cloud generated by a set of continuous frames (which we call continuous frame groups) of coronary angiogram. The six subgraphs (a-e) in this figure represent 3D point clouds generated by six different frame groups. The smaller the number of points in different 3D point clouds, the worse the performance of 3D point clouds (the higher the quality coefficient, the lower the quality).

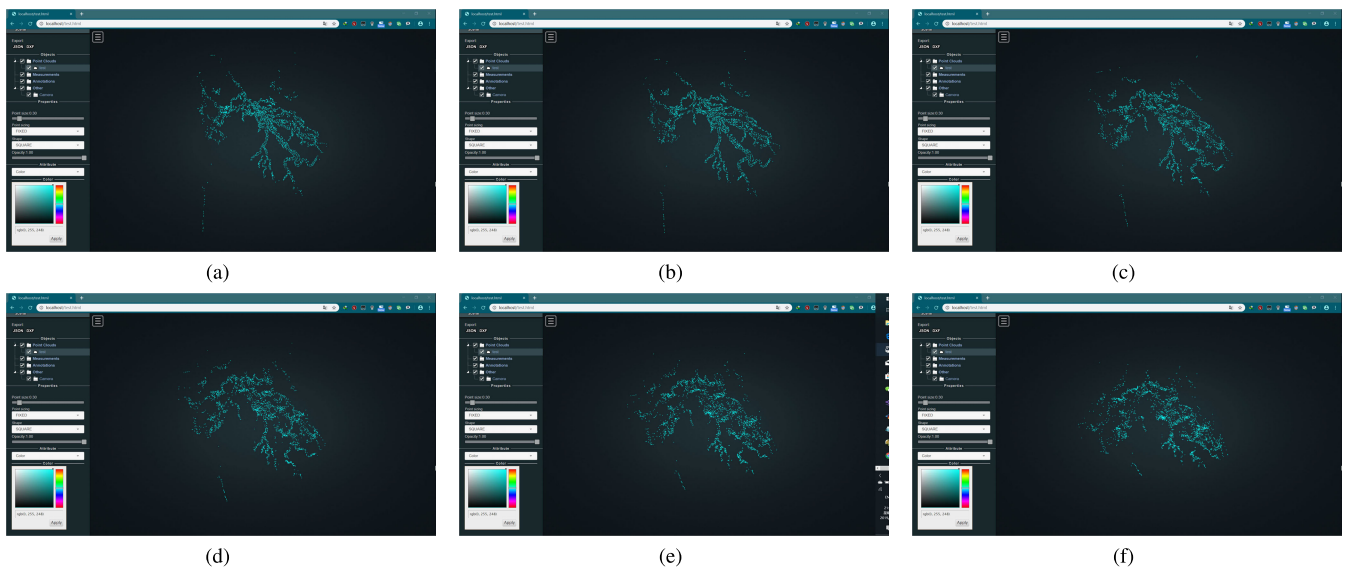


**FIGURE 7.** The final result show on the web-level platform “Potree”. The six subgraphs(a-f) represent the performance of the same 3D point cloud rotating around the Y axis at six different angles.

reconstruction methods. However, our methods’ disadvantages are very obvious, the accuracy of 3D data is relatively

low and the rendering performance is weak. In the future, filters that are more suitable for point cloud three-dimensional

reconstruction can be used to reduce noise, thereby improving the quality of extracting two-dimensional feature points. 3D point cloud generated by the optical flow method can also filter the noise by combining the midline and OCT images, or optimize the position of the points in the point cloud to improve the display performance. Moreover, 3D point cloud model generated now can also reconstruct the mesh models through suitable surface reconstruction techniques.

## VII. CONCLUSION

In this paper, we propose a method for constructing a 3D medical organ model based on the optical flow method and apply it to the reconstruction of 3D coronary arteries. The method uses coronary angiogram as input data and a 3D point cloud as output data. The resulting 3D coronary artery point cloud can work well on the web side and the results are satisfactory. However, what is even more exciting for us is the enormous potential of the optical flow method for 3D medical model reconstruction. Most of medical videos are two-dimensional, which provides a broad space for the construction of 3D models based on optical flow methods.

## REFERENCES

- [1] *World Health Statistics 2016: Monitoring Health for the SDGs Sustainable Development Goals*. World Health Org., Geneva, Switzerland, 2016.
- [2] S. L. Duce, J. R. Weir-McCall, S. J. Gandy, S. Z. Matthew, D. B. Cassidy, L. McCormick, P. Rauchhaus, H. Looker, H. M. Colhoun, and J. G. Houston, "Cohort comparison study of cardiac disease and atherosclerotic burden in type 2 diabetic adults using whole body cardiovascular magnetic resonance imaging," *Cardiovascular Diabetol.*, vol. 14, no. 1, 2015, Art. no. 122.
- [3] G. Cennamo, M. R. Romano, M. A. Breve, N. Velotti, M. Reibaldi, G. Cennamo, and G. de Crecchio, "Evaluation of choroidal tumors with optical coherence tomography: Enhanced depth imaging and OCT-angiography features," *Eye*, vol. 31, no. 6, pp. 906–915, 2017.
- [4] A. Furman, R. Riestenberg, A. Pawlowski, D. Schneider, D. M. Lloyd-Jones, and M. J. Feinstein, "Abstract P189: Factors associated with stenosis on invasive coronary angiography for persons living with human immunodeficiency virus (PLWH): The HIV electronic comprehensive cohort of CVD complications (HIVE-4CVD)," *Circulation*, vol. 137, p. AP189, Mar. 2018.
- [5] V. Vigneshwaran, G. B. Sands, I. J. LeGrice, B. H. Smaill, and N. P. Smith, "Reconstruction of coronary circulation networks: A review of methods," *Microcirculation*, vol. 26, Jul. 2019, Art. no. e12542.
- [6] I. O. Andrikos, A. I. Sakellarios, P. K. Siogkas, P. I. Tsompou, V. I. Kigka, L. K. Michalis, and D. I. Fotiadis, "A novel method for 3D reconstruction of coronary bifurcation using quantitative coronary angiography," in *World Congress on Medical Physics and Biomedical Engineering*. Singapore: Springer, 2019, pp. 191–195.
- [7] S. Çimen, A. Gooya, M. Grass, and A. F. Frangi, "Reconstruction of coronary arteries from X-ray angiography: A review," *Med. Image Anal.*, vol. 32, pp. 46–68, Aug. 2016.
- [8] A. Polańczyk, M. Strzelecki, T. Woźniak, W. Szubert, and L. Stefańczyk, "3D blood vessels reconstruction based on segmented ct data for further simulations of hemodynamic in human artery branches," *Found. Comput. Decis. Sci.*, vol. 42, no. 4, pp. 359–371, 2017.
- [9] A. F. Frangi, W. J. Niessen, K. L. Vincken, and M. A. Viergever, "Multiscale vessel enhancement filtering," in *Proc. Int. Conf. Med. Image Comput. Comput.-Assisted Intervent.* Berlin, Germany: Springer, 1998, pp. 130–137.
- [10] J. V. B. Soares, J. J. G. Leandro, R. M. Cesar, H. F. Jelinek, and M. J. Cree, "Retinal vessel segmentation using the 2-D Gabor wavelet and supervised classification," *IEEE Trans. Med. Imag.*, vol. 25, no. 9, pp. 1214–1222, Sep. 2006.
- [11] T. Jerman, F. Pernuš, B. Likar, and V. Z. Špiclin, "Beyond Frangi: An improved multiscale vesselness filter," *Proc. SPIE*, vol. 94132A, Mar. 2015, Art. no. 94132A.
- [12] T. Coye, "A novel retinal blood vessel segmentation algorithm for fundus images," MATLAB Central File Exchange, Jan. 2017. [Online]. Available: <https://www.mathworks.com/matlabcentral/fileexchange/50839-novel-retinal-vessel-segmentation-algorithm-fundus-images>
- [13] R. Van Uitert and I. Bitter, "Subvoxel precise skeletons of volumetric data based on fast marching methods," *Med. Phys.*, vol. 34, no. 2, pp. 627–638, 2007.
- [14] F. Galassi, M. Alkhalil, R. Lee, P. Martindale, R. K. Kharbanda, K. M. Channon, V. Grau, and R. P. Choudhury, "3D reconstruction of coronary arteries from 2D angiographic projections using non-uniform rational basis splines (NURBS) for accurate modelling of coronary stenoses," *PLoS ONE*, vol. 13, no. 1, 2018, Art. no. e0190650.
- [15] A. Banerjee, F. Galassi, E. Zacur, G. L. De Maria, R. Choudhury, and V. Grau, "Point-cloud method for automated 3D coronary tree reconstruction from multiple non-simultaneous angiographic projections," *IEEE Trans. Med. Imag.*, 2019.
- [16] C. Chiastra, E. Montin, M. Bologna, S. Migliori, C. Aurigemma, F. Burzotta, S. Celi, G. Dubini, F. Migliavacca, and L. Mainardi, "Reconstruction of stented coronary arteries from optical coherence tomography images: Feasibility, validation, and repeatability of a segmentation method," *PLoS ONE*, vol. 12, no. 6, 2017, Art. no. e0177495.
- [17] H. H. Khaleel, R. O. K. Rahmat, D. M. Zamrin, R. Mahmud, and N. Mustapha, "3D surface reconstruction of coronary artery trees for vessel locations' detection," *Arabian J. Sci. Eng.*, vol. 39, no. 3, pp. 1749–1773, 2014.
- [18] D. Zhang, N. Xie, S. Liang, and J. Jia, "3D tree skeletonization from multiple images based on PyrLK optical flow," *Pattern Recognit. Lett.*, vol. 76, pp. 49–58, Jun. 2016.
- [19] J. Shi, "Good features to track," in *Proc. IEEE Conf. Comput. Vis. Pattern Recognit.*, Jun. 1994, pp. 593–600.
- [20] C. G. Harris and M. Stephens, "A combined corner and edge detector," in *Proc. Alvey Vis. Conf.*, vol. 15, no. 50, pp. 10–5244, 1988.
- [21] J.-Y. Bouguet, "Pyramidal implementation of the affine lucas Kanade feature tracker description of the algorithm," *Intel Corp.*, vol. 5, nos. 1–10, p. 4, 2001.
- [22] C. Huang, W. Zhou, Y. Lan, F. Chen, Y. Hao, Y. Cheng, and Y. Peng, "A novel WebVR-based lightweight framework for virtual visualization of blood vasculum," *IEEE Access*, vol. 6, pp. 27726–27735, 2018.

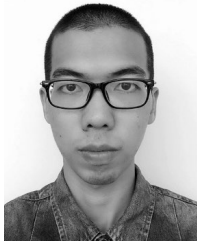


**CHANG LIU** received the Ph.D. degree, in 2019. He has been at the School of Information Engineering, Nanchang Hangkong University, Nanchang, China, where he is currently a Lecturer. His research interests include medical images analysis, WebVR visualization, virtual reality, and deep learning. He is a member of ACM and Chinese Computer Federation (CCF).



**ZHAO ZHANG** was born in Handan, Hebei, China, in 1999. He is currently pursuing the bachelor's degree in educational technology (game software development) with Nanchang Hangkong University.

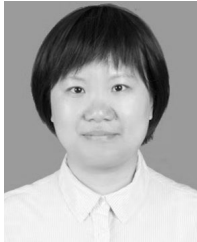




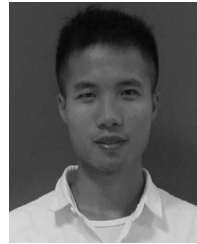
**HUANGXING LIN** received the B.S. degree in tracking technology and instrument from Beijing Jiaotong University, in 2015, and the M.S. degree in control theory and control engineering from Xiamen University, Xiamen, China, in 2018, where he is currently pursuing the Ph.D. degree in signal and information processing. His research interests include MRI Reconstruction, medical image segmentation, and machine learning.



**YIFAN LU** received the B.Ec. degree in instructional technology from Nanchang Hangkong University, Nanchang, China, in 2019. He is currently pursuing the M.Eng. degree with the University of Electronic Science and Technology of China. His current research interests include computer graphics, game engine, and deep learning.



**YAQIONG HU** received the bachelor's degree in nursing from the Shanghai University of Traditional Chinese Medicine, in 2015. She is currently a Supervisor Nurse with Shanghai East Hospital, catheterization laboratory in China. Her research interests include image reconstruction and nursing of catheterization laboratory.



**XIN DAI** was born in Xinyu, Jiangxi, China, in 1997. He is currently pursuing the bachelor's degree with Nanchang Hangkong University, majoring in educational technology (game software development).

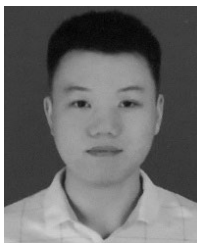


**EYK NG** received the Ph.D. degree from Cambridge University. His expertise is in commercial and in-house developed software to perform numerical simulation in the biomedical engineering (BME), thermal-fluid, and health-related diagnosis fields. He has been recognized internationally for academic excellence. He is a Fellow of the American Society of Mechanical Engineers (FASME) and a member of Academy of Pedagogy and Learning, USA. He has been an

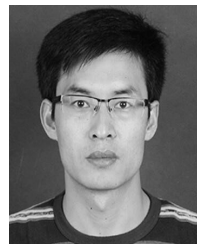
Editorial Board Member for ten journals and reviewer for 30 journals. He received a Cambridge Commonwealth Scholarship for his Ph.D. degree. He received the SPRING-Singapore Merit Award for his work in thermal imagers to screen SARS fever as well as contributions to the Singapore Standardization Program. He was the Editor-in-Chief for two ISI-journals which were captured by the JCR within two years of their inauguration. He is an expert research funding reviewer for many funding agencies worldwide.



**SHIPU XU** received the M.Sc. degree in computer science from Jiangxi Agricultural University, Nanchang, China, in 2009, where he is currently pursuing the Ph.D. degree. His research interests include image processing, data fusion, machine learning, and the agricultural Internet of Things.



**DANGZHAO CHEN** was born in Sanming, Fujian, China, in 1998. He is currently pursuing the bachelor's degree with Nanchang Hangkong University, majoring in educational technology (game software development).



**XIAOJUN LIU** received the Ph.D. degree, in 2018. He is currently a Lecturer in computer science with the Nanhu College of Jiaying University, Jiaying, China. He is also a member of ACM and Chinese Computer Federation (CCF). His research interests include 3D medical modeling, medical data analysis, 3D graphics, and machine learning.



**LEI ZHAO** received the bachelor's degree from Nanchang Hangkong University, in 2018. He is currently pursuing the degree with the University of Electronic Science and Technology of China. His research interests include 3D graphics, deep learning, and machine learning.



**NING XIE** received the M.E. and Ph.D. degrees from the Department of Computer Science, Tokyo Institute of Technology, Tokyo, Japan, in 2009 and 2012, respectively. In 2012, he was appointed as a Research Associate with the Tokyo Institute of Technology. Since 2017, he has been an Associate Professor with the School of Computer Science and Engineering, UESTC. His research interests include computer graphics, game engine, and the theory and application of artificial intelligence and machine learning. His research is supported by research grants, including NSFC, China, MOE, China, CREST, Japan, and The Ministry of Education, Culture, Sports, Science and Technology, Japan.

...